

Prediction of cavitation over hydrofoil using RANS based models

Barani Ilango Balan

B. Tech in Mechanical Engineering

Manipal Institute of Technology, Manipal

Under the guidance of

Dr Sathi Rajesh Reddy

Department of Mechanical Engineering, Shiv Nadar University, Delhi

Pranay Pandey

FOSSEE, IIT Bombay, Mumbai

Abstract

This study presents a numerical investigation of cavitation over a NACA 0012 hydrofoil using the interPhaseChangeFoam solver in OpenFOAM. The hydrofoil, with a chord length of 0.1 m, is simulated in a C-type computational domain created in Gmsh. A two-phase homogeneous mixture model is employed along with the Schnerr & Sauer cavitation model to capture vapor formation and collapse. The k- ϵ turbulence model is used to resolve turbulent effects, and mesh refinement near the hydrofoil surface ensures accurate boundary layer resolution. Simulations are carried out for two cases: steady cavitation at 4° angle of attack and cavitation number $\sigma = 0.8$, and unsteady cloud cavitation at 7° angle of attack and $\sigma = 0.7$. The results reveal the initiation and development of cavitation from the leading edge, and the transition to cloud cavitation due to re-entrant jets.

1. Introduction

Cavitation is a phenomenon which is mostly in observed pumps, ship impellers and in hydrofoils as well. Cavitation takes place when the local pressure drops below the vapour pressure of the fluid, during the process of cavitation there is formations of vapour bubbles at the site of cavitation which is known as nucleation sites. These vapour bubbles travel downstream and collapse once the local pressure is above the vapour pressure of the fluid. When the bubble collapses there is a formation of strong pressure waves along with jets which causes large number of forces on the surface of an object. This is the cause of erosion in devices where water is the working fluid.

Cavitation can be classified its form. Sheet cavitation appears as a continuous vapour layer that forms on the suction side of the hydrofoil. It is typically attached to the surface and can be steady or evolve into unsteady forms. When the sheet cavity is in the unsteady form it can break off from the surface into cloud cavitation. Cloud cavitation is characterized by the shredding of large vapour clusters which get convected downstream causing strong pressure pulses. Another type of cavitation is known as bubble cavitation which forms isolated, discrete vapor bubbles that form and collapse independently. Each type of cavitation has distinct flow characteristics and consequences, influencing performance, noise, and potential damage in hydraulic machinery and marine applications

2. Problem Statement

We are going to simulate the phenomenon of cavitation over a hydrofoil using the interPhaseChangeFoam solver. The hydrofoil used in this simulation is the NACA 0012 airfoil with a chord of 0.1m.

3. Governing Equations

In this study, cavitation flow is modelled using a homogeneous mixture model, treating the fluid–vapor mixture as a single phase with variable density based on pressure. The mixture continuity equation and momentum equation are shown below.

Continuity Equation

$$\frac{\partial(\rho_m)}{\partial t} + \nabla \cdot (\rho_m \vec{v}_m) = 0 \quad (1)$$

Momentum Equation

$$\frac{\partial(\rho_m u_i)}{\partial t} + \frac{\partial(\rho_m u_j u_i)}{\partial x_j} = \frac{\partial}{\partial x_j} \left[\mu_m \left(\frac{\partial u_i}{\partial x_j} + \frac{\partial u_j}{\partial x_i} \right) \right] - \frac{\partial p}{\partial x_i} + \frac{2}{3} \mu_m \frac{\partial u_k}{\partial x_k} + \rho_m g_i + \frac{\partial R_{ij}}{\partial x_j} \quad (2)$$

The mixture density is defined as follow

$$\rho_m = \rho_l \alpha_l + \rho_v (1 - \alpha_l) \quad (3)$$

Where ρ_l and ρ_v are the liquid and vapour densities respectively; α_l and α_v are the liquid fraction and vapour fractions respectively

For modelling turbulence in the flow, The k- ε turbulence model was used in this simulation.

The transport equation for the turbulent kinetic energy k is:

$$\frac{\partial}{\partial t} (\rho k) + \nabla \cdot (\rho U k) = \nabla \cdot (\rho D_k \nabla k) + \rho G - \frac{2}{3} \rho k (\nabla \cdot U) - \rho \beta^* \omega k + S_k \quad (4)$$

The transport equation for rate of dissipation of turbulent kinetic energy ε :

$$\frac{\partial(\rho \varepsilon)}{\partial t} + \text{div}(\rho \varepsilon U) = \text{div} \left(\frac{\mu_t}{\sigma_\varepsilon} \text{grad } \varepsilon \right) + C_{1\varepsilon} \frac{\varepsilon}{k} 2\mu_t S_{ij} S_{ij} - C_{2\varepsilon} \rho \frac{\varepsilon^2}{k} \quad (5)$$

For cavitation modelling the Schnerr & Sauer cavitation model was used for this simulation.

The vapour fraction is obtained using the equation shown below.

$$\frac{\partial(\alpha \rho_v)}{\partial t} + \nabla \cdot (\alpha \rho_v \vec{v}) = R_e - R_c \quad (6)$$

Where the terms R_e and R_c represent the evaporation and condensation term which are computed using the equations given by Schnerr & Sauer.

When the local pressure is below the vapour pressure ie. $P \leq P_v$

$$R_e = \frac{\rho_v \rho_l}{\rho} \alpha (1 - \alpha) \frac{3}{R_B} \sqrt{\frac{2(P_v - P)}{3\rho_l}} \quad (7)$$

When the local pressure is above the vapour pressure ie. $P \geq P_v$

$$R_c = \frac{\rho_v \rho_l}{\rho} \alpha (1 - \alpha) \frac{3}{R_B} \sqrt{\frac{2(P - P_v)}{3\rho_l}} \quad (8)$$

Where P_v is the vapour pressure of the fluid, R_B is the bubble radius which can be related to α and bubble density number n_b as mentioned below.

$$R_B = \left[\left(\frac{\alpha}{1 - \alpha} \right) \left(\frac{3}{4\pi n_b} \right) \right]^{1/3} \quad (9)$$

4. Simulation Procedure

4.1 Geometry and Mesh

The computational domain and the hydrofoil were created using the open-source software called gmsh. The computational domain is C shaped domain adopted from the paper by Chen et al [1]. The domain dimensions are defined with a total length of $11C$, where C represents the chord length of the hydrofoil. The upstream section extends $6C$ from the hydrofoil's leading edge, and the downstream section extends $5C$ from the trailing edge. The height of the domain is $8C$, providing sufficient space to capture the flow field around the hydrofoil.

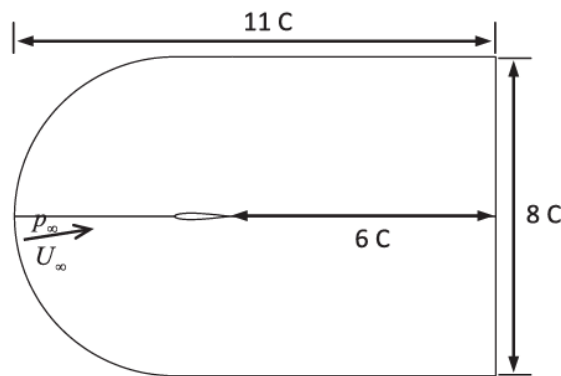


Figure 1 Fluid Domain

Special attention was given to the near-wall meshing, where inflation layers (prismatic layers) were introduced to resolve the viscous sublayer and accurately capture the boundary layer profiles. The wake region behind the hydrofoil was also refined to adequately capture vortex

shedding and potential cavitation structures. Far-field boundaries were meshed coarsely to reduce computational cost while maintaining solution accuracy. Due to the limitation of computational resource the mesh independent study was not conducted and a coarse mesh was used for this study.

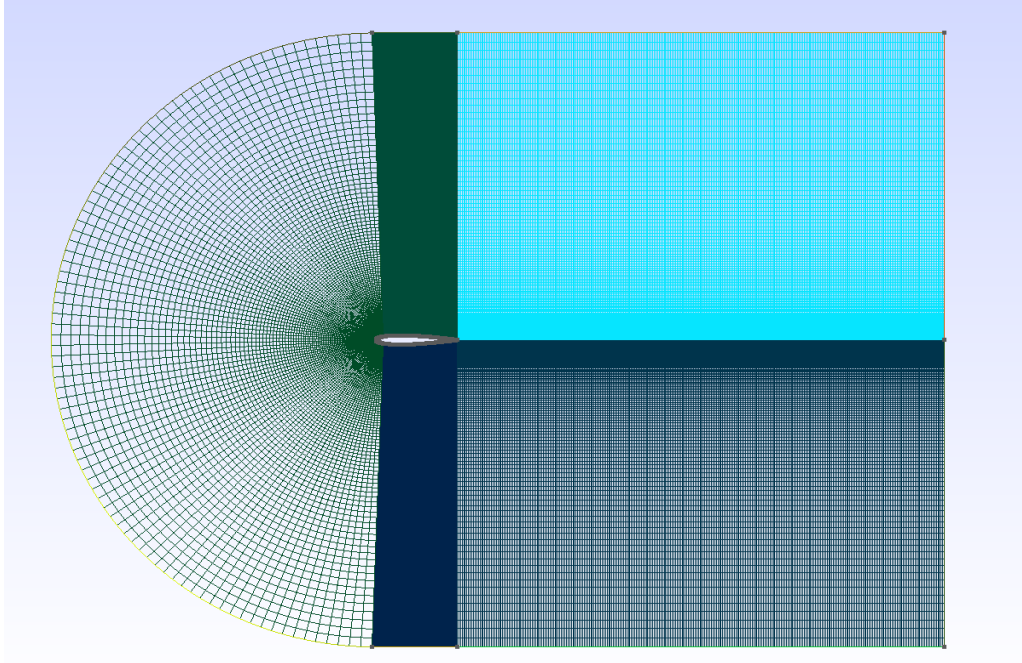


Figure 2 Mesh of the computational domain

4.2 Initial and Boundary Conditions

The mesh is converted from gmsh format to Openfoam format using the “gmshToFoam” command, this will create the polymesh folder inside the constant folder. The hydrofoil surface is changed from patch to wall and the front and back are changed from patch to empty. For cavitation simulation a non cavitating flow field is computed using the pimpleFoam solver before the interPhaseChangeFoam solver is used to compute the cavitating flow field. The Boundary conditions used for the patches are shown in the table below.

Table 1: Boundary conditions

Boundary name	U	P	P_rgh	k	ε	ω
inlet	17 m/s at 4° AOA	zerogradient	zerogradient	1.083	1.45	14.87
outlet	zerogradient	0	Calculated using cavitation formula	zerogradient	zerogradient	zerogradient
hydrofoil	noslip	zerogradient	zerogradient	kqRWallFu nction	epsilonWall Function	omegaWall Function
front and back	empty	empty	empty	empty	empty	empty
Top and bottom	zerogradient	zerogradient	zerogradient	zerogradient	zerogradient	zerogradient

During the cavitation simulation, the outlet pressure was changed accordingly using the cavitation number formula.

$$\sigma = \frac{P_{\infty} - P_v}{\frac{1}{2}\rho V^2} \quad (10)$$

Where σ : Cavitation number

P_{∞} : Free stream (ambient) pressure,

ρ : Fluid density

V : Free-stream velocity

4.3 Solver

Two solver were employed for this simulation pimpleFoam and interPhaseChangeFoam. The pimpleFoam solver is a transient solver for incompressible, turbulent flow of single-phase fluids using the PIMPLE algorithm (merged PISO-SIMPLE). In this simulation pimpleFoam is used to calculate the non cavitating flow field, which ensures numerical stability, accurately locates the cavitation-prone regions, and improves convergence in the subsequent cavitating simulation. The cavitation field is then computed using the interPhaseChangeFoam

solver. It is a two-phase, incompressible solver in OpenFOAM based on the Volume of Fluid (VOF) method. It models phase change phenomena like evaporation and condensation using cavitation models like Zwart, Schnerr&Sauer, Kunz etc. The solver captures the interface between liquid and vapor while accounting for mass transfer across phases

5. Results and Discussions

The simulations were carried out in two different flow conditions to study the steady and unsteady cavitation effects over the hydrofoil. The result for each case is shown below.


Case-1: 4° Angle of attack with cavitation number of 0.8

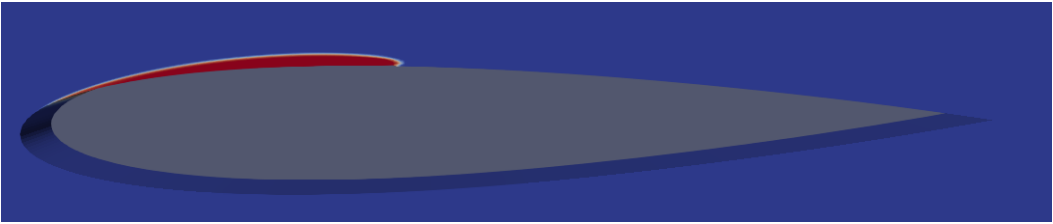

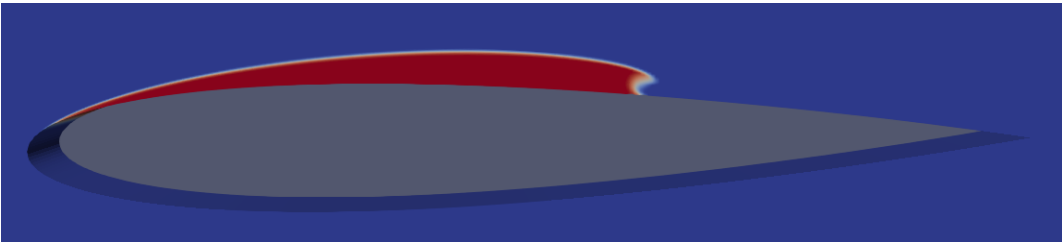
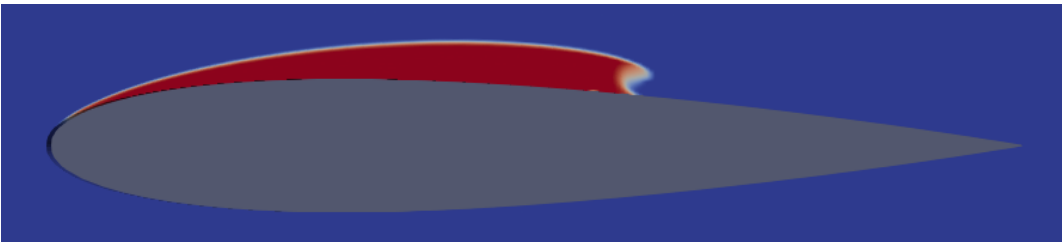
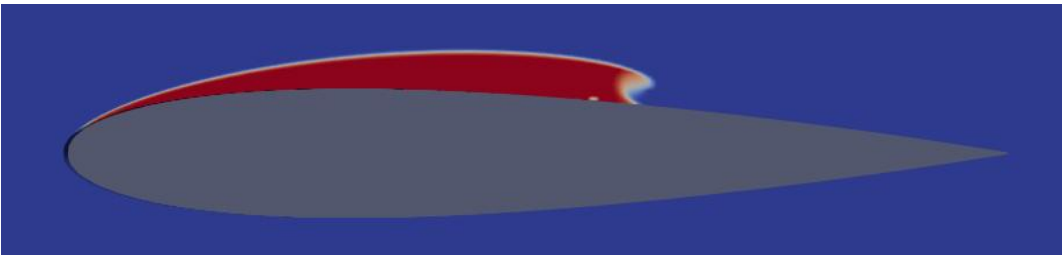
Steady cavitation refers to the cavitation sheet which nearly constant in size leading to a persistent cavity typically anchored at the leading edge or specific low-pressure regions.

- The entire flow time was 0.115s with a timestep of $5e-5$ s to keep the courant number <1 .
- The cavitation initiated in the upper surface of the leading edge in the regions where <https://www.youtube.com/watch?v=-oXCMFX9H8g> The Time taken to reach steady cavitation was $T=0.105$ s.

The vapour fraction contours presented in Table 2 illustrate the evolution and steady-state behaviour of cavitation on the hydrofoil surface over various flow times, providing a visual representation of the cavitation sheet's development. Steady cavitation, as depicted, refers to a persistent cavity that remains nearly constant in size, typically anchored at the leading edge or other low-pressure regions of the hydrofoil.

Table 2: Vapour Fraction Contours for steady cavitation for various flowtime

Time	Vapour Fraction Contour
0.2T	


0.4T	 A flow visualization around a teardrop-shaped airfoil at a time step of 0.4T. The airfoil is dark grey, and the background is dark blue. A red, elongated wake is visible behind the airfoil, indicating the region of high vorticity or velocity deficit.
0.6T	 A flow visualization around a teardrop-shaped airfoil at a time step of 0.6T. The red wake has grown in length and intensity compared to the 0.4T time step.
0.8T	 A flow visualization around a teardrop-shaped airfoil at a time step of 0.8T. The red wake continues to expand and its structure becomes more complex.
T	 A flow visualization around a teardrop-shaped airfoil at a time step of T. The red wake is at its maximum extent, showing a well-defined vortex structure.
1.1T	 A flow visualization around a teardrop-shaped airfoil at a time step of 1.1T. The red wake is still prominent, though it appears slightly more dispersed than at the previous time step.

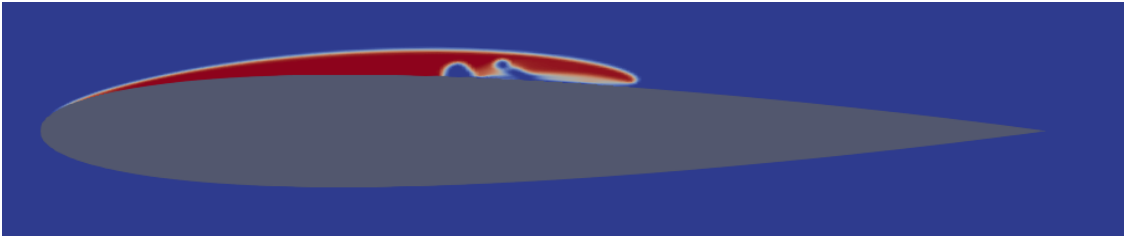
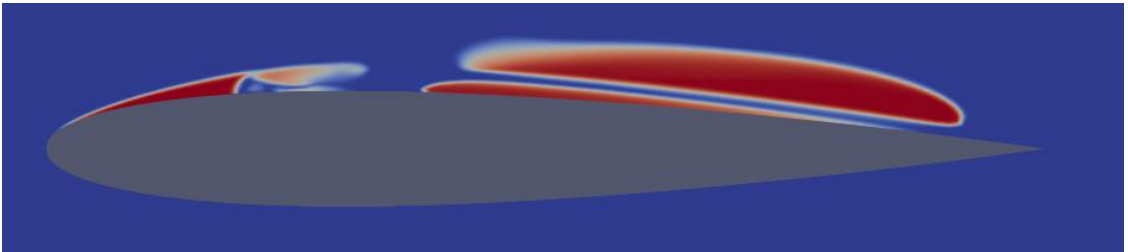
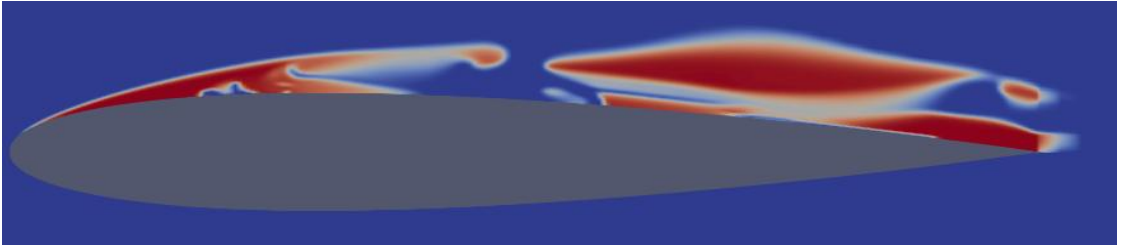
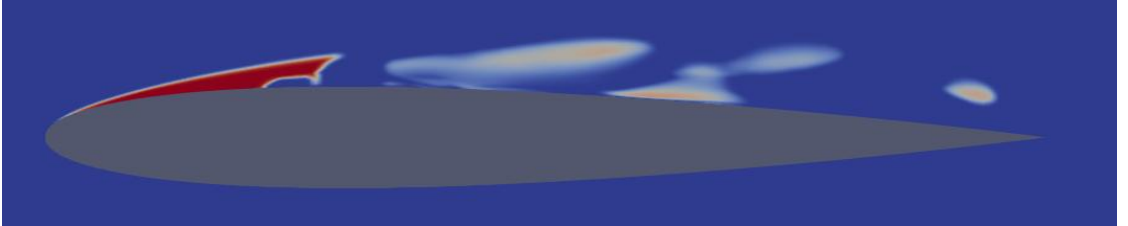

Case-2: 7° Angle of attack with cavitation number of 0.7

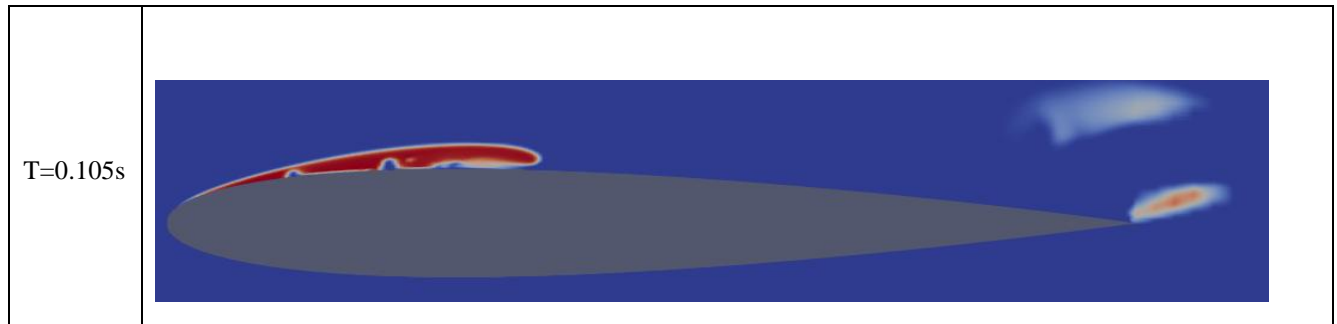
Unlike steady cavitation, sheet cavitation in unsteady regimes separates from the hydrofoil surface due to the action of re-entrant jets. When the sheet cavity grows beyond half the chord length, a cloud-like bubbly mixture detaches from its rear, forming what is known as cloud cavitation. This detached cloud strengthens as it moves downstream, splitting the low-pressure region into two distinct zones. Meanwhile, the original sheet cavity near the leading edge shrinks due to the high pressure at the cavity closure, leaving behind only a small sheet cavity. The cloud cavitation continues to grow while traveling through the low-pressure region, eventually collapsing in the wake. After the collapse, the sheet cavity begins to regrow, and the cycle repeats.

The vapour fraction contours presented in Table 3 illustrates the Vapour fraction contours at different flow times showing the transient evolution of cavitation over the hydrofoil. The contours illustrate how cavitation initiates as a sheet cavity near the leading edge, which subsequently grows and detaches due to re-entrant jet action. This detachment leads to the periodic shedding of vapour structures, followed by collapse in the downstream region. The sequence across time highlights the inherently unsteady nature of the cavitation process, distinguishing it from steady cavitation behaviour.

Table 3: Vapour Fraction Contours for unsteady cavitation for various flow time

Time	Vapour fraction contour
0.2T	

0.4T	 A flow visualization around a grey airfoil on a blue background. A single, elongated red region representing a vortex is attached to the upper surface of the airfoil.
0.6T	 The flow visualization at 0.6T shows the red vortex region beginning to detach from the upper surface of the airfoil, with some internal structure visible.
0.75T	 At 0.75T, the red vortex region has detached from the airfoil and is moving away, showing a more complex, elongated shape.
0.8T	 At 0.8T, the red vortex region is further detached and appears to be breaking apart into smaller, more irregular structures.
0.9T	 At 0.9T, the flow is mostly smooth and blue, with only a small, faint red region remaining near the leading edge of the airfoil, indicating the vortex has dissipated.



6. Conclusion

This study successfully demonstrated the numerical prediction of cavitation phenomena over a NACA 0012 hydrofoil using OpenFOAM's interPhaseChangeFoam solver. The results captured the initiation, growth, and collapse of vapor cavities for both steady and unsteady regimes, highlighting the transition from attached sheet cavitation to cloud cavitation under varying operating conditions

Acknowledgement

I am sincerely grateful to the FOSSEE team for providing me with the invaluable opportunity to participate in the Summer Fellowship program. I would like to express my heartfelt thanks to my guide, **Dr. Satish Rajesh Reddy**, for his continuous support, guidance, and encouragement throughout the project. His expertise in Computational Fluid Dynamics greatly enhanced my understanding of these complex topics and inspired me to delve deeper into the field. I am also thankful to my mentor, **Mr. Pranay Pandey**, for his insightful suggestions, practical advice, and consistent mentorship, especially in navigating OpenFOAM and the overall simulation workflow.

References

- [1] Y. Chen, X. Chen, Z. Gong, J. Li, and C. Lu, "Numerical investigation on the dynamic behavior of sheet/cloud cavitation regimes around hydrofoil," *Appl. Math. Model.*, vol. 40, no. 11–12, pp. 5835–5857, 2016, doi: 10.1016/j.apm.2016.01.031.
- [2] M. Zhao, D. Wan, and Y. Gao, "Comparative study of different turbulence models for cavitation flows around naca0012 hydrofoil," *J. Mar. Sci. Eng.*, vol. 9, no. 7, 2021, doi: 10.3390/jmse9070742.